ADVANCED MATERIALS INTERFACES
www.advmatinterfaces.de

Assembly of Advanced Materials into 3D Functional Structures by Methods Inspired by Origami and Kirigami: A Review

*Xin Ning, Xueju Wang, Yi Zhang, Xinge Yu, Dongwhi Choi, Ning Zheng, Dong Sung Kim, Yonggang Huang, Yihui Zhang, and John A. Rogers**

Origami and kirigami, the ancient techniques for making paper works of art, also provide inspiration for routes to structural platforms in engineering applications, including foldable solar panels, retractable roofs, deployable sunshields, and many others. Recent work demonstrates the utility of the methods of origami/kirigami and conceptually related schemes in cutting, folding, and buckling in the construction of devices for emerging classes of technologies, with examples in mechanical/optical metamaterials, stretchable/conformable electronics, micro/nanoscale biosensors, and large-amplitude actuators. Specific notable progress is in the deployment of functional materials such as single-crystal silicon, shape memory polymers, energy-storage materials, and graphene into elaborate 3D micro and nanoscale architectures. This review highlights some of the most important developments in this field, with a focus on routes to assembly that apply across a range of length scales and with advanced materials of relevance to practical applications.

1. Introduction

Origami involves the folding of 2D sheets to create 3D objects;[1–4] kirigami is a variant of origami that exploits additional degrees of freedom offered by cuts in these sheets to expand the range of accessible 3D geometries.[5–8] Due to their shape-adaptive nature, origami and kirigami, originally applied only to paper, can serve as routes to large-scale structural systems that require packaging and deployment, such as foldable solar panels,[9,10] retractable roofs,[11] deployable sunshields,[12] and many others.[13] More recent work demonstrates that these and related methods for assembling planar materials into complex 3D structures can exploit sophisticated 2D fabrication technologies and thin film materials from the electronics/optoelectronics industries, to yield functional systems in 3D designs that were previously unachievable.[14–18] In this way, the techniques of origami/kirigami can enable many classes of nontraditional devices not only at the macroscale but also at the micro/nanoscale, with the potential to open up opportunities for unusual engineering designs in microsystems technologies.[19–22]

Much research in origami/kirigami assembly aims to extend the range of length scales and the scope of functional materials that can be realized in 3D systems, and to transfer those ideas and

Dr. X. Ning
Department of Materials Science and Engineering
Frederick Seitz Materials Research Laboratory
University of Illinois at Urbana-Champaign
Urbana, IL 61801, USA
Dr. X. Wang, Dr. Y. Zhang, Dr. X. Yu
Simpson Querrey Institute and Feinberg Medical School
Center for Bio-Integrated Electronics
Northwestern University
Evanston, IL 60208, USA
Dr. D. Choi,[+] Prof. D. S. Kim
Department of Mechanical Engineering
Pohang University of Science and Technology (POSTECH)
Gyeongbuk 790-784, South Korea
N. Zheng
State Key Laboratory of Chemical Engineering
College of Chemical and Biological Engineering
Zhejiang University
Hangzhou 310027, P. R. China
The ORCID identification number(s) for the author(s) of this article can be found under https://doi.org/10.1002/admi.201800284.
[+]Present address: Department of Mechanical Engineering, Kyung Hee University, Yongin 17104, South Korea
Prof. Y. Huang
Departments of Civil and Environmental Engineering, Mechanical Engineering, and Materials Science and Engineering
Northwestern University
Evanston, IL 60208, USA
Prof. Y. Zhang
Center for Mechanics and Materials
AML
Department of Engineering Mechanics
Tsinghua University
Beijing 100084, P. R. China
Prof. J. A. Rogers
Departments of Materials Science and Engineering, Biomedical Engineering, Neurological Surgery, Chemistry, Mechanical Engineering, Electrical Engineering and Computer Science
Simpson Querrey Institute and Feinberg Medical School
Center for Bio-Integrated Electronics
Northwestern University
Evanston, IL 60208, USA
E-mail: jrogers@northwestern.edu

DOI: 10.1002/admi.201800284

concepts into important applications. Recent trends suggest a shift from assembly based on applied force and external actuation[23–25] to contact-free, self-folding of active materials that are responsive to external stimuli.[16,26,27] Additional progress is in expanding the range of constituent materials from passive, structural materials, to high-performance, multifunctional materials needed for functional systems in photovoltaics,[28,29] energy-storage,[30–32] electronics,[22,33–35] and chem/biosensing.[36–38] Broad classes of functional devices and systems with mechanical, electrical, biomedical, and other types of functionality are now beginning to appear, with examples in mechanical metamaterials,[23,24,39,40] soft robotics,[41–43] stretchable/flexible electronics,[14,19,30,44,45] and functional scaffolds for tissue engineering.[46,47]

This paper reviews the most recent advances in origami/kirigami and related forms of assembly, with emphasis on schemes that allow deployment of advanced materials in 3D functional structures with a wide range of length scales, from macroscale to microscale and nanoscale. The discussion begins with the techniques and applications of macroscale origami and kirigami enabled by external actuation and self-folding. Subsequent sections summarize approaches to assembly that exploit the mechanics of compressive buckling in ways that are compatible with broad classes of advanced functional materials and 2D microsystems technologies across length scales. A final section highlights recent work on sub-micrometer scale structures and materials. The article concludes with a summary of opportunities, challenges, and directions for future research.

2. External Actuation

Actuation[23–25] based on external forces to induce stretching, bending, and folding represents the simplest means to assemble structures by origami/kirigami. Recent research establishes means for exploiting this simple approach to create macroscale functional 3D structures for engineering applications that are not possible to realize using traditional methods. Reconfigurable architectures achieved in this way are of particular interest. This section highlights some of the most notable recent examples, with a focus on mechanical metamaterials and stretchable, flexible electronics, as shown in **Figure 1**.

2.1. Mechanical Metamaterials

Mechanical metamaterials that employ structural design to achieve exotic and tunable material properties are of rapidly growing interest.[24,39,48–50] The shape-morphing capabilities of structures formed by origami/kirigami are ideal for metamaterials that offer reconfigurable structural layouts and properties. The top panel in Figure 1a shows an origami tube derived from the Miura-ori pattern that is assembled into a stiff and yet reconfigurable metamaterial.[51] This structure couples rigidly foldable origami tubes in a "zipper" manner that allows only one degree-of-freedom of axial deployment via manual application of a force on any point. The effective stiffness is high by comparison for any other mode of bending or twisting. Transformable metamaterials with multiple degrees of freedom are also possible, as shown in the middle panel of Figure 1a.[52]

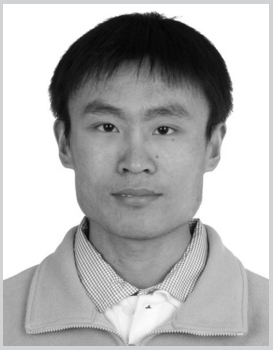

Xin Ning is currently a postdoctoral research associate in the Department of Materials Science and Engineering at the University of Illinois at Urbana-Champaign working with Professor John A. Rogers. He received his PhD in Aeronautics from the California Institute of Technology in 2015 under the guidance of Professor Sergio Pellegrino. Dr. Ning received his Master of Science in Aeronautics from Caltech in 2010. He was a Dow-Resnick Fellow in the Resnick Sustainability Institute at Caltech. He received his Bachelor of Engineering in Aircraft Design and Engineering from Beihang University in China in 2009.

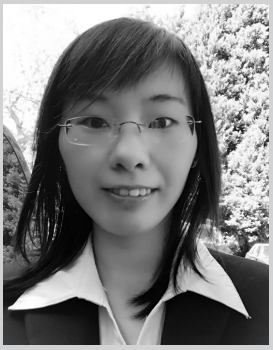

Xueju Wang received her B.E. in Chemical Engineering from the Dalian University of Technology, China in 2011. She received her Ph.D. degree in Mechanical Engineering from the Georgia Institute of Technology, Atlanta, Georgia, USA in 2016. She is currently a postdoctoral scholar in Materials Science and Engineering at Northwestern University. Her research interests are mechanics, materials, and structures for energy storage and human health, involving multiple physical processes at the nanometer and micrometer length scales.

John A. Rogers is the Louis Simpson and Kimberly Querrey Professor of Materials Science and Engineering, Biomedical Engineering and Neurological Surgery at Northwestern University. Dr. Rogers completed his Ph.D. at Massachusetts Institute of Technology in 1995, studying physical chemistry. He was a junior fellow in the Harvard University Society of Fellows and in 1997 joined Bell Laboratories where he became Director of the Condensed Matter Physics Research Department. He was a faculty member at the University of Illinois at Urbana-Champaign from 2003–2016, after which he took his current position among the faculty at Northwestern University.

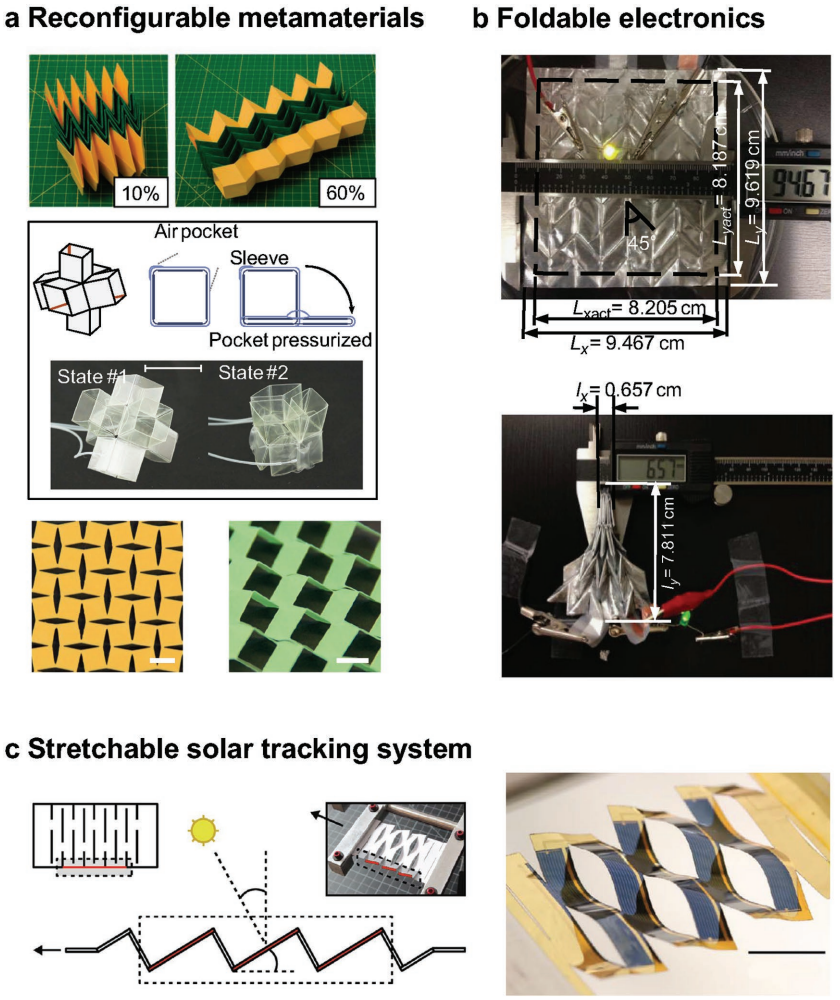

Figure 1. Macroscale origami/kirigami structures enabled by external actuation. a) Programmable and reconfigurable metamaterials by the techniques of origami/kirigami. (Top) An origami-based metamaterial that can deform into various shapes at different folding stages. Adapted with permission.[51] Copyright 2015, National Academy of Sciences. (Middle) Pneumatically actuated, origami-inspired transformable metamaterial with multiple degrees of freedom. Scale bar, 3 cm. Adapted with permission.[52] Copyright 2016, The Authors published by Springer Nature. (Bottom) Kirigami-based metamaterial. Scale bars, 6 mm. Adapted with permission.[57] Copyright 2017, American Physical Society. b) Lithium-ion batteries with origami designs: (top) deployable battery; (bottom) folded battery that powers an LED. Adapted with permission.[30] Copyright 2014, Springer Nature. c) Solar tracking system with a kirigami design. (Left) Schematic illustration showing that stretching the structure enables tracking. (Right) Representative system with photovoltaic cells. Scale bar, 10 mm. Adapted with permission.[29] Copyright 2015, The Authors published by Springer Nature.

This example combines a modular collection of rigid faces and hinges with a scheme for pneumatic actuation to transform between various configurations. In addition to reconfigurable shape and volume, this system also offers tunable stiffness, achieved by active switching among its stable states. Origami assembly can also realize important basic architectural elements in mechanical metamaterials with other unusual properties, such as negative Poisson's ratio,[23,48,53] bistability,[54] self-locking,[55] and controllable thermal expansion.[56]

Kirigami provides an alternative approach to mechanical metamaterials. The bottom panel of Figure 1a shows examples formed by kirigami with orthogonal cuts.[57] Strategically designing the thicknesses of the constituent 2D sheets allows realization of diverse mechanical properties when the structures are under tensile deformation. When the thickness is sufficiently large, the kirigami structure deforms in the plane, resulting in a metamaterial with negative Poisson's ratio. By contrast, when the thickness is small, the structure forms a complex, buckled 3D geometry, thereby providing a simple route for manufacturing complex 3D structures out of flat sheets. The design freedom offered by kirigami also creates opportunities for other forms of mechanical metamaterials such as hierarchical auxetic metamaterials with high stretchablity[58] and shape morphing kirigami metamaterials.[40,59]

2.2. Stretchable/Flexible Electronics

The shape-adaptive capabilities of structures formed by origami/kirigami provide an interesting route to stretchable/flexible electronics, complementing approaches that use stretchable structures (e.g., serpentine interconnection and pop-up bridges)[60–63] or stretchable materials (e.g., stretchable conductive lines of single-walled carbon nanotubes.[64,65] Figure 1b highlights a foldable lithium-ion battery that uses an origami design,[30] where the top panel shows the deployed configuration and the bottom one presents the folded battery, as it powers an light-emitting diode (LED). This device uses a classical Miura-ori folding pattern to achieve significant linear and areal deformability, twistability, and bendability without compromising the energy storage capability. Related principles in origami design serve as the basis for other classes of stretchable and flexible devices, such as deformable silicon solar cells,[28] paper photodetector arrays,[66] foldable antennas,[45] and many others.[32,44]

The out-of-plane deformations associated with kirigami structures under external actuation can yield other classes of 3D tunable systems. Figure 1c shows a dynamic kirigami structure for integrated solar tracking.[29] The tracker in this case consists of linear patterns of cuts in thin, flexile materials. Stretching the kirigami sheet in the axial direction induces controlled buckling into a 3D geometry with tunable angle of inclination. Integrating thin photovoltaic materials onto this simple platform yields a photovoltaic system with operating characteristics that match those of conventional, complex trackers. Similar ideas can be used in soft deployable reflectors for optical beam steering.[67] Other work shows that kirigami structures can serve as structural platforms for stretchable/flexible electronics, such as carbon nanotube-embedded stretchable conductors,[68] stretchable batteries,[31] and triboelectric nanogenerators.[69]

3. Self-Folding of Stimuli-Responsive Materials

Processes of self-folding of stimuli-responsive materials bypass needs for external actuation in origami/kirigami assembly. Such materials have characteristics, such as shape, mechanical moduli, permeability, or optical properties,[70–77] that change in response to variations in temperature, light, pH, electric field, or solvent. These systems are of long-standing interest for applications in sensors and actuators,[78] robotics,[79,80] deployable objects,[81] and implantable devices.[82] Two types of stimuli-responsive materials that have received intense attention over last decade are shape memory polymers (SMPs) and hydrogels, due to their ability to change in shape and/or volume, over a wide range in a reversible, controllable manner. Recent studies indicate that the shape morphing characteristics of these materials or of their heterogeneous combinations with other classes of materials can enable interesting routes to the origami/kirigami assembly.[83] This section reviews recent advances in this area, including shape manipulation and sequential self-folding through the action of SMPs and digitally printed 3D hydrogel structures.

3.1. Shape Memory Polymer Structures

SMPs are stimuli-responsive polymers that can recover their original (or permanent) shape upon exposure to external stimuli.[70,71,84] These materials have been explored in morphing aircraft technology,[85] platforms for controlled drug release,[86] minimally invasive medical devices,[87] and many others. The development of SMPs with sophisticated and controllable shape-changing capabilities is critically important to the field. In addition to traditional irreversible dual-shape memory polymers, recent efforts include two-way reversible SMPs[88,89] and multi shape memory polymers.[90–92] The traditional shape-changing behavior of SMPs follows from the storage and release of entropic energy via chain conformation changes in SMPs (elasticity of SMPs), and is therefore recoverable.[84,93–95] Such elastic behavior can, however, enable only a temporary shape fixing of SMPs. A recent advance in realizing complex shape manipulation uses thermally distinct elasticity and plasticity in SMPs.[96] In such SMPs, permanent shape changes occur through dynamic covalent bond exchange within the polymer network (plasticity of SMPs), which allows its topography to rearrange in response to an external force. In this way, a single polymer that integrates elasticity and plasticity at distinct temperatures can realize complex changes in shape.

Figure 2a shows 3D shape manipulations of SMPs by using thermally distinct plasticity and elasticity. A square film consists of a cross-linked poly(caprolactone) system with a melting transition temperature of 55 °C, which is also the shape memory transition temperature. A transesterification catalyst introduces thermal plasticity into the network, resulting in a plasticity temperature of 130 °C. The film can fold plastically into a permanent bird shape due to bond exchange above the plasticity temperature. This shape can further deform into a plane or a flat film as temporary shapes that can subsequently recover upon heating above its transition temperature. Likewise, the recovered bird can morph into a different permanent origami structure such as a boat, which can also maintain other recoverable temporary shapes such as a windmill or a flat film. In addition to origami, SMP structures with sophisticated permanent kirigami shapes can also be obtained.[97] These dynamic shape-changing behaviors provide versatile means for fabricating geometrically complex multifunctional devices.

3.2. Sequential Self-Folding

In addition to shape manipulation, spatiotemporal control during the origami/kirigami assembly process is also of great interest because many processes such as DNA folding, packaging, and locomotion involve sequential events.[98–103] Existing solutions for sequential shape transformation localize an external stimulus onto selected regions of responsive materials by using focused light[103] or Joule heaters,[101,102] and pattern two or more materials that are responsive to the same stimulus but with different degrees of response.[98,99] A relatively simple strategy for sequential self-folding of 2D polymer sheets into 3D configurations uses external light.[100] Here, 2D printed patterns of colored ink define hinges on prestrained polymer sheets made of clear inkjet shrink film (Grafix). The colored ink absorbs light at different wavelengths, resulting in heating of the underlying polymer across the thickness of the sheet in a geometry defined by color of the illuminating light. The result causes self-folding of the film (0.3 mm thick) as a result of heat-induced (for temperatures above the ≈105 °C transition of this material) shrinkage (up to ≈55%).[93]

Figure 2b depicts the sequential folding of nested boxes. This example uses green and orange hinges patterned on 2D shapes that define a small and large box, respectively. Upon exposure to light from a red LED, only the green hinges absorb light, thereby inducing folding of the small box. The larger box with orange hinges starts to fold when exposed to light from a blue LED. The patterns of color temporally and spatially control the folding process. This type of shape programming may have applications in areas such as reconfigurable electronics, actuators, sensors, implantable devices, smart packaging, and deployable structures.

3.3. Printed Hydrogel Structures

In addition to SMPs, hydrogels are another type of interesting stimuli-responsive, shape-morphing materials.[74] Hydrogels, which are water-swollen polymeric materials, have an interesting combination of properties in stimuli sensitivity, biocompatibility, softness, and ability for rapid diffusion of molecules.[104,105] Hydrogels find widespread use in the human body[106] for drug delivery, fluid control, separation, and sensing. Various techniques can be used to form 3D hydrogel architectures, including direct molding,[107] "Lego" assembly,[108] 3D printing,[109,110] and emerging methods of 4D printing.[111,112] Figure 2c shows a recently developed technique for ultrafast digital printing of hydrogels.[113] The printing setup consists of a commercial projector and two

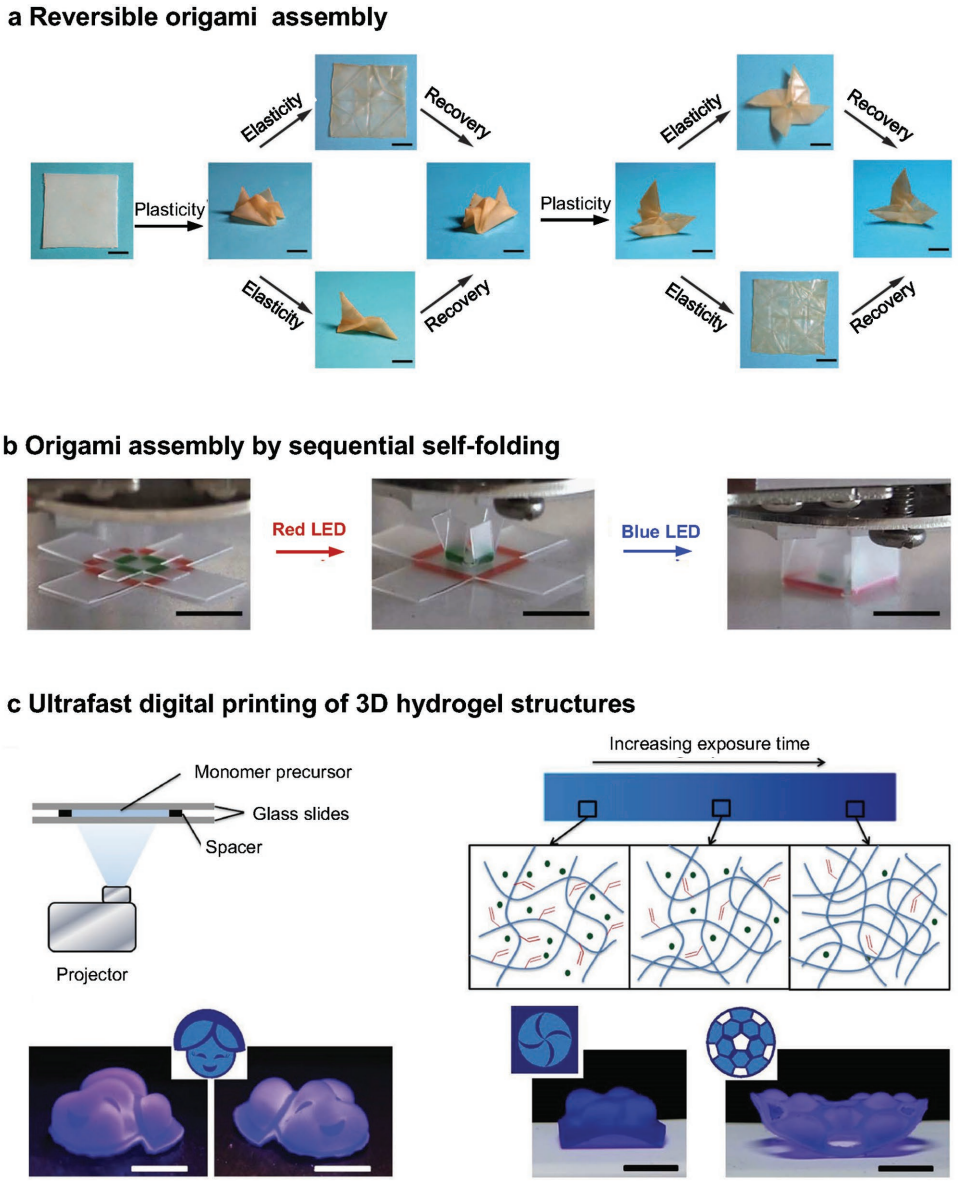

Figure 2. Macroscale origami/kirigami structures enabled by self-folding of stimuli-responsive materials. a) Smart origami structures via thermally distinct elasticity and plasticity in the constituent polymer material. Scale bars, 10 mm. Adapted with permission.[96] Copyright 2016, AAAS. b) Programmed self-folding of 2D polymer sheets into 3D origami/kirigami structures in a sequential manner using colored ink printed at the hinges and exposure to light. Adapted with permission.[98] Copyright 2017, AAAS. c) Experimental printing setup, principle, and printed multiscale buckled structures for ultrafast digital printing of 3D hydrogel structures. The insets present the planar layouts of the printed patterns. Scale bars, 1 cm. Adapted with permission.[113]

glass slides separated with a spacer (0.5 mm in thickness). The digital projector spatially controls the time of light exposure at each pixel level to create polymer networks between the two glass slides with different cross-linking densities. When immersed in water, the cross-linked polymer sample swells in a differential manner, which induces stresses that transform the 2D film into a 3D object. Figure 2c summarizes various 3D hydrogel structures fabricated with this technique, including a 3D cartoon face, a dome array, and a partially cutout 3D structure with honeycomb-shaped domes. This digital printing method can be used with other shape changing materials such as SMPs as well.

4. Assembly by Compressive Buckling

Recent work shows that alternative approaches to 3D assembly can follow from mechanics-guided methods in nonlinear buckling, as a means for deterministically transforming various planar material structures into 3D architectures that resemble those formed by origami/kirigami methods described previously.[114–117] Key advantages are compatibility with 1) the most advanced classes of materials that are available in thin film form, including soft polymers, metals, monocrystalline semiconductors, and their heterogeneous combinations, 2) state-of-the-art techniques in micro/nanofabrication used in the

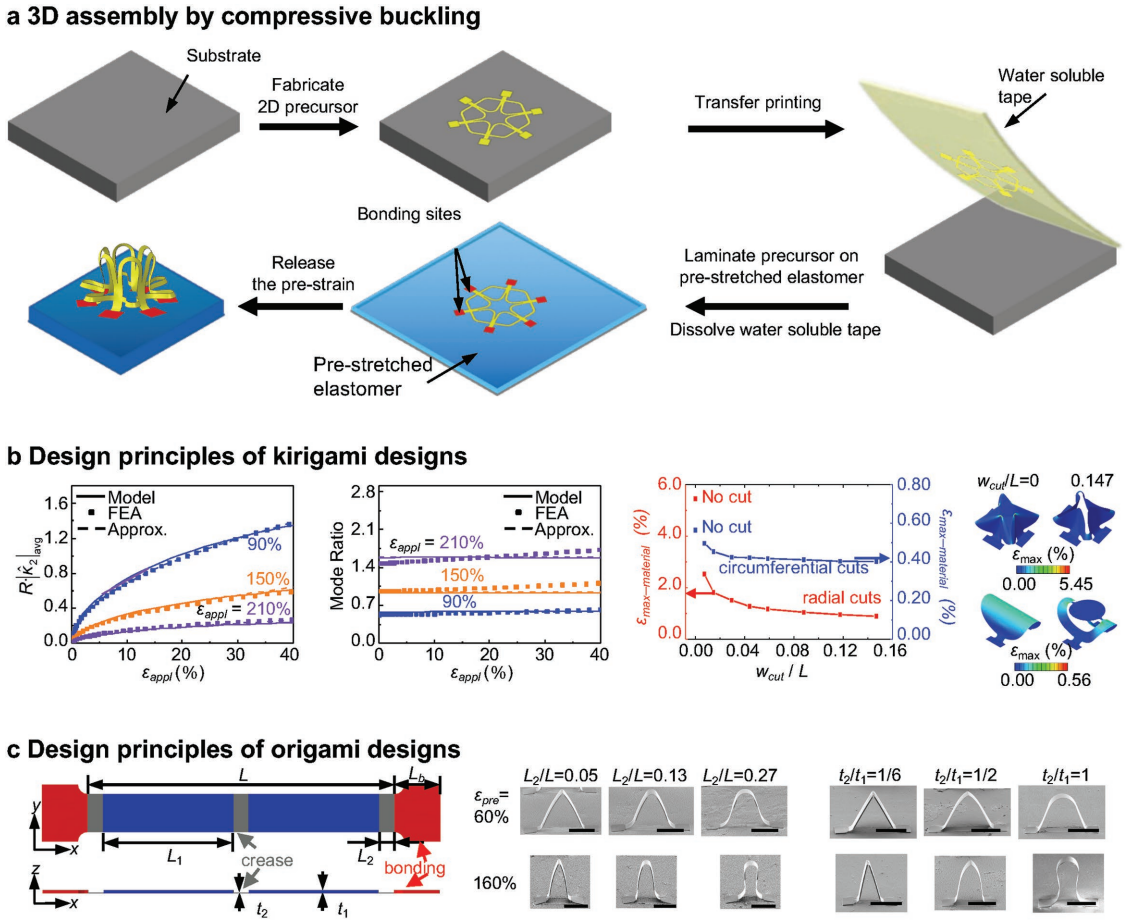

Figure 3. Multiscale origami/kirigami structures enabled by compressive buckling: fabrication and design principles. a) Schematic illustration of the process for forming 3D structures by compressive buckling. b) Influence of key geometric parameters in a class of kirigami-inspired ribbon mesostructures (with helical shapes) on the bending curvature (left) and mode ratio (middle), according to the results of model calculation, approximate solution, and FEA. The right panel shows the maximum material strain of a class of kirigami-inspired membrane mesostructures as a function of the dimensionless widths of kirigami cuts. The color in the FEA results corresponds to the magnitude of the maximum principal strain. Adapted with permission.[115] Copyright 2015, National Academy of Sciences. c) A nonuniform thickness design enables origami self-assembly: schematic illustration and scanning electron microscopy (SEM) images of deformed mesostructures consisting of bilayers of metal (Au) and polymer (SU8) under two different levels (60% and 160%) of prestrain, for nonuniform ribbons with varying length ratios (L_2/L; with $t_2/t_1 = 1/4$) or thickness ratios (t_2/t_1; with $L_2/L = 0.05$). Scale bars, 200 μm. Adapted with permission.[116]

semiconductor industry, and 3) a broad range of length scales and feature sizes, from centimeters to nanometers. This section reviews the underlying fabrication processes and design principles, with illustrations in broad classes of 3D structures and unusual devices.

4.1. Steps for Fabrication

Figure 3a describes the key steps associated with this mechanics-guided 3D assembly approach. The process begins with the formation of a 2D precursor on an underlying sacrificial layer to facilitate subsequent release from a planar supporting substrate. This precursor can incorporate any class of thin film material, patterned and processed using a broad range of techniques, including the most sophisticated used in the production of electronic, optoelectronic, and other microsystems technologies. Removing the sacrificial layer allows for release and transfer of the precursor to a water-soluble tape. Patterning the backside of the precursor defines a set of regions with surface chemistries selected to promote adhesion to a stretched elastomer substrate. In Figure 3a, the red squares indicate these bonding sites. Releasing the elastomer causes it to return to its undeformed state, thereby imposing compressive stresses on the precursor at these sites. The result leads to delamination and upward, out-of-plane movement of the nonbonded regions (described as yellow regions in Figure 3a), in a coordinated set of translational and rotational motions. This process geometrically transforms the 2D precursor into a 3D shape, in a rapid, parallel assembly process. Representative 3D structures with layouts that resemble those that can be achieved by origami/kirigami but formed in heterogeneous combinations of advanced materials patterned with lithographically controlled precision appear in Section 5, followed by their applications.

4.2. Mechanics Design

For kirigami-inspired designs, the key design variables are the geometry of the 2D precursor structures, the positions of cuts defined in them, the pattern of sites for selective bonding, and the magnitude and orientation of prestrain in the elastomer assembly platform.[114,115] Quantitative mechanics simulations based on finite element analysis (FEA) can capture all of these effects, with precise, quantitative agreement with experiment measurements. For ribbon-shaped kirigami mesostructures, analytical models of postbuckling that provide direct correlation between the final 3D geometry and the initial 2D layout can be derived through a double perturbation method[118] and an energetic method.[119] These models allow accurate predictions of the 3D configurations, curvature components, as well as the maximum strain during compressive buckling, all without the computational overhead of FEA. As an example, Figure 3b (left) shows that the analytical model predicts that the average bending curvature in a helical mesostructure has a square root dependence on the magnitude of the prestretch in the assembly platform, in agreement with FEA results. The resulting maximum strain in the mesostructure can be kept below the fracture limit of the material by optimizing the parameters associated with the process. Figure 3b (middle) demonstrates the strain-independence of a key parameter, referred to as the mode ratio that serves as a metric to classify ribbon-shaped 3D mesostructures according to their degree of bending and bending-twisting modes of deformation. By leveraging the analytical models of postbuckling, an inverse design can be achieved for relatively simple classes of 3D topologies based on helical configurations. The development of similar capabilities in inverse modeling for arbitrary systems represents an area for future work.

Deformations of membrane-shaped kirigami mesostructures involve an increased level of complexity,[115] suitable for quantitative description only by FEA. Previous studies suggest that the introduction of kirigami-style cuts can suppress localized "kink" deformations that can otherwise occur, thereby creating access to an expanded breadth of 3D geometries. An example appears in Figure 3b (right). In the assembly process, material fracture represents an important failure mode, especially with systems that incorporate brittle materials (e.g., single-crystal silicon). Since the maximum strain typically follows a proportional dependence on the thickness of the 2D precursor, a reduction of thickness can help to ensure structural integrity. Although the development of inverse design strategies is quite challenging, recent work based on topology optimization suggests methods for defining patterns of cuts in 2D membranes to realize buckling-driven assembly of 3D structures with certain desired geometries.[120]

Introduction of controlled variations in thicknesses across the 2D precursor allows for formation of folding creases at desired locations in the corresponding 3D structure,[121] as essential to realization of origami-inspired architectures. As schematically shown in Figure 3c (left), a 2D precursor can include engineered, spatial modulations in thickness to guide folding deformations at specific, targeted locations. Here, both the ratio of thicknesses in the thin and thick regions (t_2/t_1) and the ratio of their lengths (L_2/L) greatly influence the deformation processes and the final 3D geometries. As shown by the results of experiments and FEA (with an example in Figure 3c, middle and right), both a small thickness ratio ($t_2/t_1 < 1/3$) and a small length ratio ($L_2/L < 0.1$) are required to induce strong folding-type deformations in the thin segments (i.e., the creases). Taken together with recently developed origami algorithms,[122,123] this approach allows access to a broad set of 3D structures, with demonstrated examples in half cylindrical columns, fish scales, cubic boxes, pyramids, skew tooth structures, soccer balls, model houses, cars, and multi floor textured buildings. To achieve elastic, reversible assembly without plastic deformations or fractures, the maximum strain should be maintained at a low level by optimizing the crease geometries and other parameters.

5. Assembly by Compressive Buckling: Structures and Applications

The design and fabrication methods described above provide versatile routes to a broad group of origami and kirigami structures at various length scales. This mechanically guided assembly approach is compatible with many advanced functional materials, including single-crystal silicon, which would be difficult or impossible to incorporating into 3D systems using other methods, thereby enabling unique devices and systems. **Figure 4** highlights the representative structures and devices created by this approach.

5.1. 3D Structures

Figure 4a shows a collection of origami structures made from various materials at sub-millimeter to centimeter scales, ranging from simple geometries to complex configurations.[35] The roof structure consists of a photo-lithographically defined polymer (SU8, MicroChem) with creases organized in the circumferential direction in an annulus. Releasing equal biaxial prestrain in the assembly substrate leads to the formation of the roof structure. This assembly approach is also compatible with composite materials. The mountain range structure is made from a bilayer of SU8 and gold, assembled by uniaxially compressing a ribbon with the creases perpendicular to its longitudinal direction. The semi-ellipsoid, box, and windmill structures incorporate a bilayer of polymer (SU8, MicroChem) and device-grade, single-crystalline silicon, to demonstrate complex origami structures from high-performance electronic materials. These origami mesostructures form through creases that form in the circumferential direction in the 2D precursors upon release of equal biaxial prestrain in their assembly substrates. Figure 4a includes two car structures with the same shapes but at different length scales. The car on the top is made from a bilayer of SU8 and gold, and its overall dimensions and characteristic feature sizes are at millimeter and micrometer scales, respectively. By contrast, the car at the bottom is made from plastic, at centimeter and millimeter scales. Other structures include pyramid, inverse pyramid, cylindrical shell, star fish, fan, soccer ball, hierarchical architectures, and many others.

In addition to engineered creases (variation in thickness) for folding, kirigami-inspired methods also include cuts (removal of materials) to obtain highly complex 3D structures.[34] Figure 4b highlights representative 3D kirigami structures assembled by compressive buckling at various length scales and from diverse

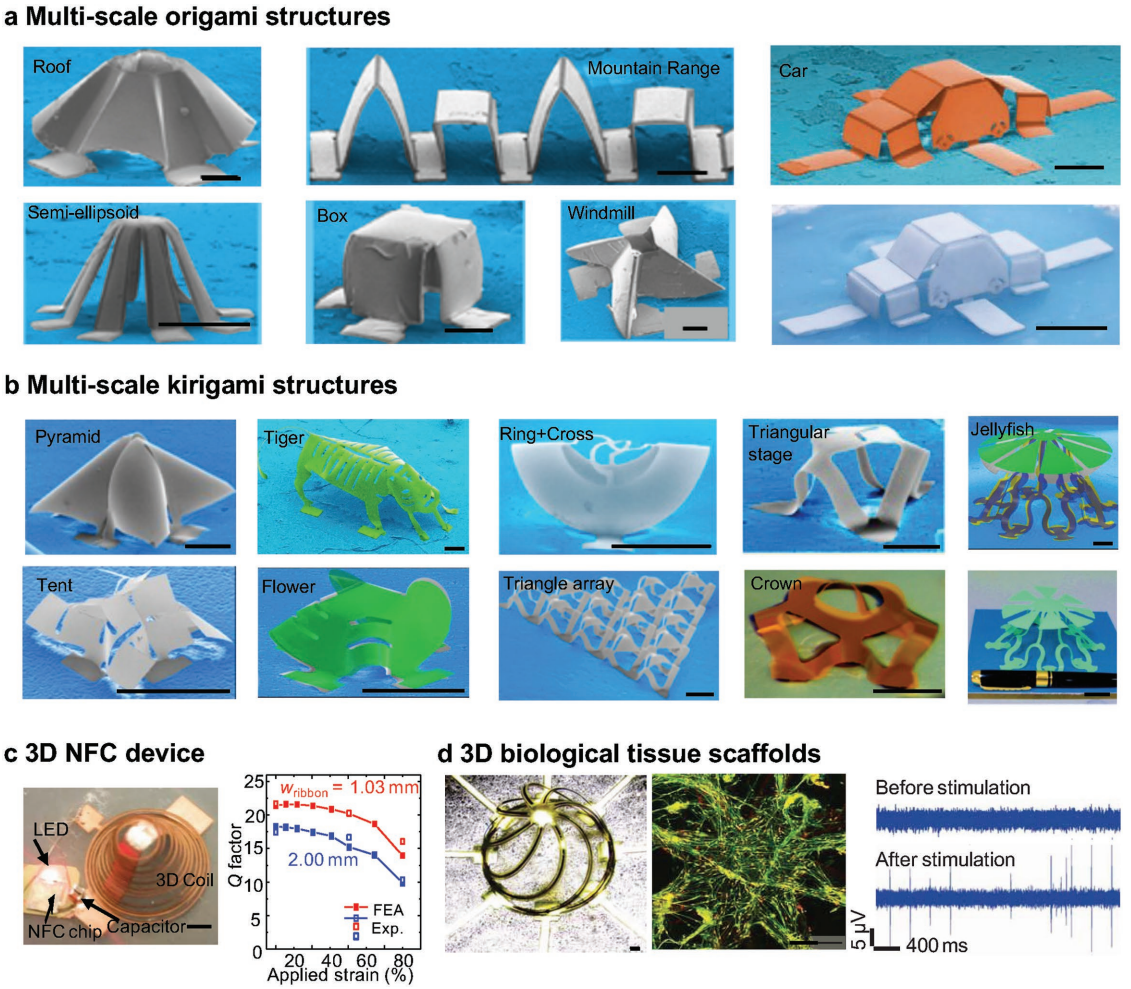

Figure 4. Mesoscale to microscale origami/kirigami structures enabled by compressive buckling: architectures and applications. a) SEM and optical images of origami structures made of various materials, such as SU8, silicon-gold, and silicon-SU8 composites. Scale bars, 200 μm (2 cm for the last one). Adapted with permission.[116] b) SEM images of various 3D kirigami structures made of various materials, such as SU8, gold, and bilayers of silicon and SU8. Scale bars, 200 μm (2 cm for the last one). Adapted with permission.[115] Copyright 2015, National Academy of Sciences, and dapted with permission.[22] Copyright 2017, Springer Nature. c) 3D NFC device for powering a red LED. Scale bars, 2 mm. Adapted with permission.[124] Copyright 2016, AAAS. d) Optical and confocal fluorescence images of a 3D cage with integrated electrodes for DRG cell culture, and extracellular action potential stimulation and recording of DRG neurons using the 3D electrodes. Scale bars, 100 μm. Adapted with permission.[47] Copyright 2017, National Academy of Sciences.

functional materials, including polymers, single-crystalline silicon, metals, and various dielectrics. The pyramid structure forms from a cross-shape with straight cuts and equal biaxial strain in the assembly substrate. Introducing second-order fractal and circular cuts can lead to structures with enhanced levels of complexity, such as the tent and the flower in Figure 4b. In addition to the layouts of the cuts, the compressive strain is an important design parameter. For example, the tiger structure in Figure 4b assembles as a result of unequal biaxial strains and fractal cuts in a 2D precursor. Figure 4b also includes structures formed from hybrid collections of membranes and ribbons (e.g., ring + cross, triangular stage, triangle array), further demonstrating the versatility of this approach. A broad range of materials can be used. For example, the pyramid and tents are made from bilayers of single-crystalline silicon and polymer, and the tiger is a pure polymer structure. The crown-shape geometry is made from gold membranes and ribbons. As before, in addition to the diversity in geometries and materials, this assembly method can yield structures at various length scales, as demonstrated by the two jellyfish structures in Figure 4b at micrometer scale (top) and another at centimeter scale (bottom).

5.2. Functional 3D Systems

The ability to integrate functional materials allows construction of active and passive devices that exploit 3D geometrical design. Figure 4c,d highlights two representative applications in electronics and tissue engineering. Figure 4c shows a near-field communication (NFC) device with 3D design that enhances the Q factor and angular operating range compared to that of conventional 2D devices.[124] The 3D coil incorporates a bilayer of copper and polyimide, and the 2D kirigami precursors include spiral cuts formed by laser processing. Plasma enhanced chemical

vapor deposition forms an encapsulating layer of SiO_2 on the copper. Selectively bonding the precursor to an assembly substrate and releasing the uniaxial prestrain create the final 3D kirigami coil, with a geometry and electrical properties optimized for this antenna application.

Mechanically stretching or compressing the assembly substrates affords a simple means for reversibly adjusting the geometries of the 3D structures. Figure 4c shows the dependence of the Q factor on strain applied to the substrate for devices that have supporting ribbons with two different widths. The results show a broad range of tunability. This same scheme in tuning can be applied to other device types as well, such as tunable spiral microinductors[33] and ultrastretchable soft electronic networks.[125] Moreover, similar ideas also enable tunable opto/mechanical systems, including micromirrors[126] with adjustable focal length, optical shutters[34] with controllable transmission values, and mechanical resonators with tunable frequencies.[127]

Biological systems are inherently 3D. 3D systems like those reported here could, therefore, serve as the basis for volumetric biointerfaces in fundamental studies or, ultimately, clinical use. In one example, mechanics-guided assembly approaches yield active, 3D cellular scaffolds. Figure 4d shows a scaffold of this type, with sensing and stimulation functions for studying and controlling the activity of Dorsal Root Ganglion (DRG) neural networks.[47] Here, a 3D cage (Figure 4d, left) integrates microelectrodes (Au/Ti) for measuring the electrophysiological behaviors of growing neural networks. First, DRG cells are directly seeded and cultured on the scaffold. After thirty-five days of growth, the DRG cells organize into networks (Figure 4d, middle) that follow the 3D geometries of the scaffold and cross over the two ribbons (shortcutting the electrodes) as well. The integrated microelectrodes enable stimulation of the cells and recording of their action potentials. The top plot in the right diagram of Figure 4d shows no measurable signals, consistent with the silent behavior during this period (culturing DRG for 7 d). Electrically stimulating the network with a microelectrode triggers neural activities, such that the resulting capacitive charging (12 spikes) can be subsequently detected by the same electrode, as shown in the bottom plot of the right diagram of Figure 4d. This 3D cell scaffold provides initial, proof-of-principle results that establish the feasibility of achieving active, biointegrated 3D systems for cell and tissue engineering.

In addition to these classes of devices, this buckling approach to assembly can be used to realize many other 3D systems, including microrobots,[47] templates for growth of functional materials at high temperatures,[47] passive frameworks for guided cell growth,[128] and tunable microbalances.[129] Future advances will leverage established manufacturing methods from the semiconductor industry and transform the resulting planar technologies into 3D systems with applications in cell/tissue engineering, biointegrated electronics, biosensing, thermal and mechanical energy harvesting, soft robotics, and many others.

6. Microscale and Nanoscale Structures

One frontier area of research is in adapting methods described in the preceding sections for use in sub-micrometer and nanoscale 3D structures, of interest due not only to their fundamental properties but also for their potential uses in cellular and sub-cellular biomedical devices,[130,131] micro-electromechanical systems,[132,133] optoelectronic components,[134] and many other.[135,136] This section reviews work in microscale and nanoscale forms of origami/kirigami, with a focus on the assembly of nanoscale films of silicon (Si) and graphene into 3D architectures.

6.1. Compressive Buckling

As discussed in Section 5, the mechanics-guided assembly approach can assemble various planar materials into 3D configurations at multiple scales. **Figure 5**a shows SEM images with overlaid FEA predictions of various sub-microscale 3D structures. For example, the "starfish" framework consists of Si ribbons with widths of ≈800 nm and thicknesses of ≈100 nm.[114] As for previously described examples, micro-origami and nano-origami structures assembled in this way have mechanically tunable 3D geometries.[114] This assembly technique enables transformation of sub-microscale planar materials into complex 3D configurations for many applications.

6.2. Graphene Origami/Kirigami

2D materials, such as graphene, molybdenum disulfide, and boron nitride, are of broad recent interest due to their unusual combination of mechanical, electrical, optical, and thermal properties.[137,138] Examples of application possibilities span stretchable/flexible electronics, energy conversion and storage, and biosensors.[139–143] The transformation of these atomically thin, planar materials into complex 3D structures by bending, wrinkling, or folding could significantly alter their mechanical, electrical, and optical properties, to create opportunities for further development of functional devices and structures.

Inspired by the techniques of origami, Figure 5b shows a thermally responsive method to reversibly fold and unfold monolayer graphene into 3D structures.[135] Here, modifying the surface of the graphene with ultrathin layers of polydopamine and thermoresponsive poly(N-isopropylacrylamide) (PNIPAM) brushes and micropatterning the resulting system allow for self-folding into ordered 3D structures as a result of temperature-induced transformations of PNIPAM from collapsed to swollen states. Increasing the temperature to ≈45 °C in aqueous media triggers the flower to fold its free petals toward the center and transform from an open to a closed state. A closed graphene flower unfolds upon cooling from 45 to 25 °C. Self-folding of modified graphene can also be used to tune the electrical properties. The current (I)–voltage (V) response in the flat state shows a linear behavior, with a well-defined sheet resistance. After folding, the I–V curve changes dramatically into a nonlinear form, due to changes in the electrical properties at the locations of the folds.

The qualitative similarity between the mechanics of paper and graphene makes it easy to translate ideas from paper models to graphene. Inspired by the techniques of kirigami, graphene can be assembled into 3D configurations under

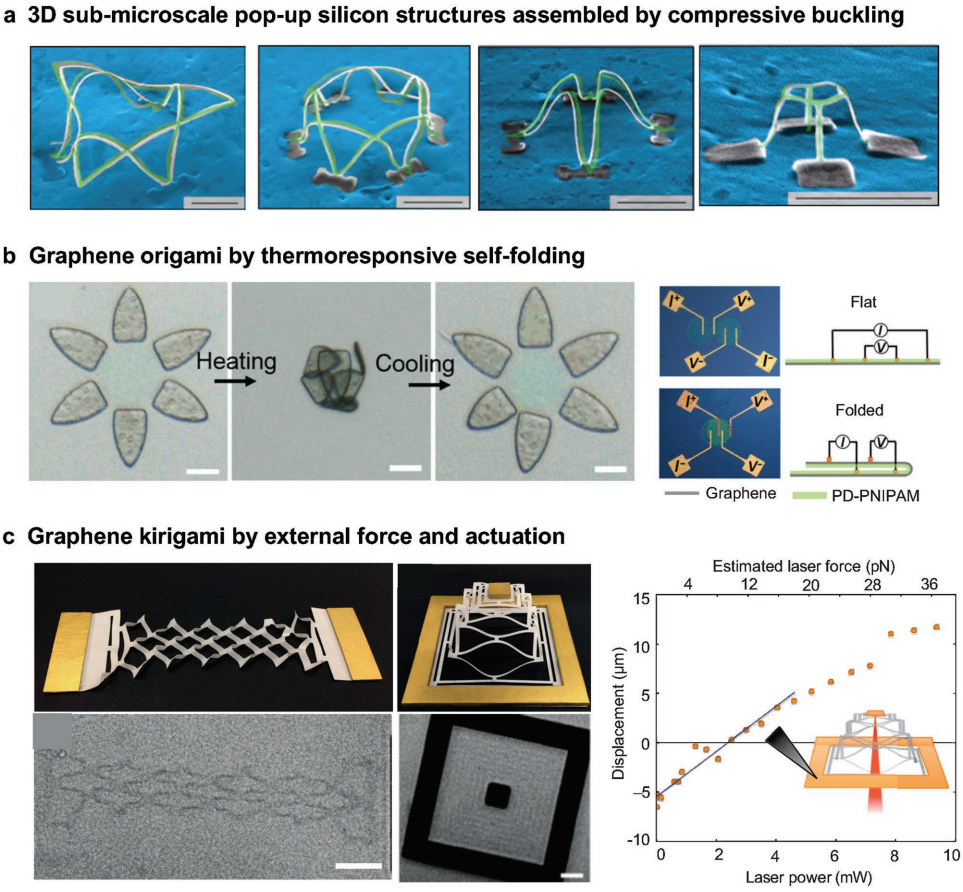

Figure 5. Origami/kirigami structures at sub-micrometer length scales. a) 3D silicon structures assembled by compressive buckling with sub-micrometer scale ribbons (widths: 800 nm; thicknesses: 100 nm). Scale bars, 15 μm. Adapted with permission.[117] Copyright 2017, AAAS. b) Reversible self-folding of graphene and its application in creased transistors. Scale bars, 50 μm. Adapted with permission.[135] Copyright 2017, AAAS. c) Stretchable graphene kirigami structure and its application in stretchable transistors. The paper models show the geometries of graphene kirigami deformed in 2D or 3D. Scale bars, 10 μm. Adapted with permission.[136] Copyright 2015, Springer Nature.

in-plane or out-of-plane loading, in a manner analogous to that of a paper model (Figure 5c).[136] Realization of kirigami-inspired shapes highlights the mechanical robustness and extremely high elongation limits (≈240%) of graphene with strategic cuts. The results foreshadow the ability to build highly stretchable transistors with graphene or other 2D materials. The conductance curves in the unstretched and stretched states show negligible differences, mainly because the graphene lattice itself does not experience significant strain during extension of the kirigami spring. Furthermore, stretching a device for more than 1000 times does not substantially change its electrical properties. The programmed folding/unfolding motions can be manipulated by mechanical stages, magnetic forces, or other externally imposed stimuli.

7. Conclusion and Outlook

Origami and kirigami, originally conceived as forms of art, are rapidly evolving into means to realize engineering applications that are difficult or impossible to achieve using other techniques. This paper reviews some of the most recent advances in origami/kirigami assembly of 3D functional structures with dimensions spanning the macroscale and the micro/nanoscale, emphasizing the assembly approaches and the application possibilities. The assembly techniques span those that use external actuation, self-folding, and compressive buckling. Constituent materials include almost every class, from hydrogels to shape–memory polymers to single crystalline inorganic semiconductors, although only certain methods, such as the mechanics-guided assembly technique, are compatible with all of them. Existing applications lie mainly in the macroscale size regime, although the ability to leverage micro/nanofabrication methods from the semiconductor industry suggests broad possibilities in microsystems technologies across a broad spectrum of fields of use.

External actuation will continue to serve as a simple yet powerful method to create functional structures by origami/kirigami at large length scales. Here, new design methods may expand the range of geometries that are possible and transform these designs into practical applications through integration of multifunctional materials and devices. Self-assembly by use of mechanically active materials, such as hydrogels and shape–memory polymers, will likely receive increasing attention. Challenges in such systems are in increasing the associated forces of actuation and response speeds, and in converting the

structural concepts into functional platforms. The difficulties in manipulating micro/nanoscale structures by external actuation have hampered the realization of complexity and functionality in origami/kirigami structures at these small scales. Therefore, advanced mechanically active materials that enable high-precision control over actuation force and displacement in this regime will be critically important in extending the frontier of functional origami/kirigami systems at micro/nanometer scales. The buckling-induced mechanical assembly techniques summarized here will find increasing opportunities in broader applications due to their versatility capabilities in materials, structure geometries and length scales. In the area of biomedicine, the complex, mesoscale 3D multifunctional devices achieved using these approaches will provide unprecedented opportunities in the development of biointegrated electronics for fundamental biomedical research and clinical medical devices. In the area of materials science, this approach affords options in the development of novel research tools for fundamental studies and of growth scaffolds for the creation of new materials. In the area of electrical engineering, new classes of 3D electronics may create design opportunities that lie beyond those possible with conventional 2D electronics. These ideas have the potential to open important research frontiers and to create unusual engineering applications in other areas, ranging from aerospace, mechanical, and civil engineering, for studies in reconfigurable structures, broadband energy harvesters, and many others.

Acknowledgements

X.N. and X.W. contributed equally to this work. The authors acknowledge the support from the U.S. Department of Energy, Office of Science, Basic Energy Sciences (# DE-FG02-07ER46471). Y.Z. acknowledges support from the National Natural Science Foundation of China (# 11672152 and # 11722217). Y.H. acknowledges the support from the NSF (# CMMI1400169, # CMMI1534120, and # CMMI1635443). This article is part of the *Advanced Materials Interfaces* Hall of Fame article series, which highlights the work of top interface and surface scientists.

Conflict of Interest

The authors declare no conflict of interest.

Keywords

3D functional structures, advanced materials, kirigami, origami

Received: February 20, 2018
Revised: March 23, 2018
Published online: May 7, 2018

[1] L. H. Dudte, E. Vouga, T. Tachi, L. Mahadevan, *Nat. Mater.* **2016**, *15*, 583.
[2] Y. Chen, R. Peng, Z. You, *Science* **2015**, *349*, 396.
[3] R. J. Lang, presented at *Proc. Bridges 2009: Mathematics, Music, Art, Architecture, Culture*, Banff, Alberta, Canada, July **2009**.
[4] R. J. Lang, presented at *Proc. Twelfth Annual Symposium on Computational Geometry*, Philadelphia, Pennsylvania, USA, May **1996**.
[5] T. Castle, D. M. Sussman, M. Tanis, R. D. Kamien, *Science Advances* **2016**, *2*, e1601258.
[6] T. Castle, Y. Cho, X. Gong, E. Jung, D. M. Sussman, S. Yang, R. D. Kamien, *Phys. Rev. Lett.* **2014**, *113*, 245502.
[7] F. Wang, X. Guo, J. Xu, Y. Zhang, C. Q. Chen, *J. Appl. Mech.* **2017**, *84*, 061007.
[8] B. G.-g. Chen, B. Liu, A. A. Evans, J. Paulose, I. Cohen, V. Vitelli, C. D. Santangelo, *Phys. Rev. Lett.* **2016**, *116*, 135501.
[9] D. Thesiya, A. R. Srinivas, P. Shukla, *J. Astron. Instrum.* **2015**, *04*, 1550006.
[10] S. A. Zirbel, B. P. Trease, M. W. Thomson, R. J. Lang, S. P. Magleby, L. H. Howell, presented at *SPIE Defense + Security*, Toulouse, France, April **2015**.
[11] S. Pellegrino, *Deployable Structures*, Vol. *412*, Springer, Berlin, Germany **2014**.
[12] L. Wilson, S. Pellegrino, R. Danner, presented at AIAA Paper, Boston, MA, USA, April **2013**.
[13] A. Lebée, *Int. J. Space Struct.* **2015**, *30*, 55.
[14] Y. Zhang, Y. Huang, J. A. Rogers, *Curr. Opin. Solid State Mater. Sci.* **2015**, *19*, 190.
[15] N. Turner, B. Goodwine, M. Sen, *Proc. Inst. Mech. Eng., Part C* **2015**, *230*, 2345.
[16] Q. Zhang, J. Wommer, C. O'Rourke, J. Teitelman, Y. Tang, J. Robison, G. Lin, J. Yin, *Extreme Mech. Lett.* **2017**, *11*, 111.
[17] T.-K. A. Chou, K. Najafi, in *Transducers '01 Eurosensors XV: The 11th Int. Conf. Solid-State Sensors and Actuators* (Ed: E. Obermeier), Springer, Berlin, Heidelberg **2001**, p. 1542.
[18] N. S. Shaar, *Vol. Doctorate*, Massachusetts Institute of Technology, **2014**.
[19] J. Rogers, Y. Huang, O. G. Schmidt, D. H. Gracias, *MRS Bull.* **2016**, *41*, 123.
[20] Z. Song, C. Lv, M. Liang, V. Sanphuang, K. Wu, B. Chen, Z. Zhao, J. Bai, X. Wang, J. L. Volakis, L. Wang, X. He, Y. Yao, S. Tongay, H. Jiang, *Small* **2016**, *12*, 5401.
[21] L. Xu, T. C. Shyu, N. A. Kotov, *ACS Nano* **2017**, *11*, 7587.
[22] Y. Zhang, F. Zhang, Z. Yan, Q. Ma, X. Li, Y. Huang, J. A. Rogers, *Nat. Rev. Mater.* **2017**, *2*, 17019.
[23] M. Eidini, G. H. Paulino, *Science Advances* **2015**, *1*, e1500224.
[24] J. L. Silverberg, A. A. Evans, L. McLeod, R. C. Hayward, T. Hull, C. D. Santangelo, I. Cohen, *Science* **2014**, *345*, 647.
[25] E. D. Demaine, T. Tachi, presented at *LIPIcs-Leibniz International Proceedings in Informatics*, Lisbon, Portugal, December **2017**.
[26] Q. Zhao, W. Zou, Y. Luo, T. Xie, *Sci. Adv.* **2016**, *2*, e1501297.
[27] A. P.-H. Edwin, J. H. Darren, J. M. Richard Jr., C. L. Dimitris, *Smart Mater. Struct.* **2014**, *23*, 094001.
[28] R. Tang, H. Huang, H. Tu, H. Liang, M. Liang, Z. Song, Y. Xu, H. Jiang, H. Yu, *Appl. Phys. Lett.* **2014**, *104*, 083501.
[29] A. Lamoureux, K. Lee, M. Shlian, S. R. Forrest, M. Shtein, *Nat. Commun.* **2015**, *6*, 8092.
[30] Z. Song, T. Ma, R. Tang, Q. Cheng, X. Wang, D. Krishnaraju, R. Panat, C. K. Chan, H. Yu, H. Jiang, *Nat Commun* **2014**, *5*, 3140.
[31] Z. Song, X. Wang, C. Lv, Y. An, M. Liang, T. Ma, D. He, Y.-J. Zheng, S.-Q. Huang, H. Yu, H. Jiang, *Sci. Rep.* **2015**, *5*, 10988.
[32] S. Choi, D. Lee, G. Kim, Y. Y. Lee, B. Kim, J. Moon, W. Shim, *Adv. Funct. Mater.* **2017**, *27*, 1702244.
[33] S. Xu, Z. Yan, K.-I. Jang, W. Huang, H. Fu, J. Kim, Z. Wei, M. Flavin, J. McCracken, Y. Huang, R. Wang, *Science* **2015**, *347*, 154.
[34] Y. Zhang, Z. Yan, K. Nan, D. Xiao, Y. Liu, H. Luan, H. Fu, X. Wang, Q. Yang, J. Wang, W. Ren, H. Si, F. Liu, L. Yang, H. Li, J. Wang, X. Guo, H. Luo, L. Wang, Y. Huang, J. A. Rogers, *Proc. Natl. Acad. Sci. USA* **2015**, *112*, 11757.
[35] Z. Yan, F. Zhang, J. Wang, F. Liu, X. Guo, K. Nan, Q. Lin, M. Gao, D. Xiao, Y. Shi, Y. Qiu, H. Luan, J. H. Kim, Y. Wang, H. Luo, M. Han, Y. Huang, Y. Zhang, J. A. Rogers, *Adv. Funct. Mater.* **2016**, *26*, 2629.

[36] Y. Morikawa, S. Yamagiwa, H. Sawahata, R. Numano, K. Koida, M. Ishida, T. Kawano, *Adv. Healthcare Mater.* **2018**, *3*, 1701100.
[37] L. Wu, C. Ma, L. Ge, Q. Kong, M. Yan, S. Ge, J. Yu, *Biosens. Bioelectron.* **2015**, *63*, 450.
[38] M. Jamal, S. S. Kadam, R. Xiao, F. Jivan, T.-M. Onn, R. Fernandes, T. D. Nguyen, D. H. Gracias, *Adv. Healthcare Mater.* **2013**, *2*, 1142.
[39] P. M. Reis, H. M. Jaeger, M. van Hecke, *Extreme Mech. Lett.* **2015**, *5*, 25.
[40] R. M. Neville, F. Scarpa, A. Pirrera, *Sci. Rep.* **2016**, *6*, 31067.
[41] L. Paez, G. Agarwal, J. Paik, *Soft Robotics* **2016**, *3*, 109.
[42] J.-H. Na, A. A. Evans, J. Bae, M. C. Chiappelli, C. D. Santangelo, R. J. Lang, T. C. Hull, R. C. Hayward, *Adv. Mater.* **2015**, *27*, 79.
[43] A. R. Deshpande, Z. T. H. Tse, H. Ren, presented at *2017 18th Int. Conf. Advanced Robotics (ICAR)*, Hong Kong, China, July **2017**.
[44] J. K. Paik, R. K. Kramer, R. J. Wood, presented at *2011 IEEE/RSJ Int. Conf. Intelligent Robots and Systems*, San Francisco, USA, September **2011**.
[45] M. Nogi, N. Komoda, K. Otsuka, K. Suganuma, *Nanoscale* **2013**, *5*, 4395.
[46] S.-H. Kim, H. R. Lee, S. J. Yu, M.-E. Han, D. Y. Lee, S. Y. Kim, H.-J. Ahn, M.-J. Han, T.-I. Lee, T.-S. Kim, S. K. Kwon, S. G. Im, N. S. Hwang, *Proc. Natl. Acad. Sci. USA* **2015**, *112*, 15426.
[47] Z. Yan, M. Han, Y. Shi, A. Badea, Y. Yang, A. Kulkarni, E. Hanson, M. E. Kandel, X. Wen, F. Zhang, Y. Luo, Q. Lin, H. Zhang, X. Guo, Y. Huang, K. Nan, S. Jia, A. W. Oraham, M. B. Mevis, J. Lim, X. Guo, M. Gao, W. Ryu, K. J. Yu, B. G. Nicolau, A. Petronico, S. S. Rubakhin, J. Lou, P. M. Ajayan, K. Thornton, G. Popescu, D. Fang, J. V. Sweedler, P. V. Braun, H. Zhang, R. G. Nuzzo, Y. Huang, Y. Zhang, J. A. Rogers, *Proc. Natl. Acad. Sci. USA* **2017**, *114*, E9455.
[48] T. A. M. Hewage, K. L. Alderson, A. Alderson, F. Scarpa, *Adv. Mater.* **2016**, *28*, 10323.
[49] T. Bückmann, M. Kadic, R. Schittny, M. Wegener, *Phys. Status Solidi B* **2015**, *252*, 1671.
[50] X. Zheng, H. Lee, T. H. Weisgraber, M. Shusteff, J. DeOtte, E. B. Duoss, J. D. Kuntz, M. M. Biener, Q. Ge, J. A. Jackson, S. O. Kucheyev, N. X. Fang, C. M. Spadaccini, *Science* **2014**, *344*, 1373.
[51] E. T. Filipov, T. Tachi, G. H. Paulino, *Proc. Natl. Acad. Sci. USA* **2015**, *112*, 12321.
[52] J. T. B. Overvelde, T. A. de Jong, Y. Shevchenko, S. A. Becerra, G. M. Whitesides, J. C. Weaver, C. Hoberman, K. Bertoldi, *Nat. Commun.* **2016**, *7*, 10929.
[53] Z. You, K. Kuribayashi, *Origami* **2009**, *4*, 117.
[54] H. Yasuda, J. Yang, *Phys. Rev. Lett.* **2015**, *114*, 185502.
[55] S. Kamrava, D. Mousanezhad, H. Ebrahimi, R. Ghosh, A. Vaziri, *Sci. Rep.* **2017**, *7*, 46046.
[56] E. Boatti, N. Vasios, K. Bertoldi, *Adv. Mater.* **2017**, *29*, 1700360.
[57] A. Rafsanjani, K. Bertoldi, *Phys. Rev. Lett.* **2017**, *118*, 084301.
[58] Y. Tang, J. Yin, *Extreme Mech. Lett.* **2017**, *12*, 77.
[59] Y. Tang, G. Lin, S. Yang, Y. K. Yi, R. D. Kamien, J. Yin, *Adv. Mater.* **2017**, *29*, 1604262.
[60] J. A. Rogers, T. Someya, Y. Huang, *Science* **2010**, *327*, 1603.
[61] D.-H. Kim, N. Lu, R. Ma, Y.-S. Kim, R.-H. Kim, S. Wang, J. Wu, S. M. Won, H. Tao, A. Islam, K. J. Yu, T.-i. Kim, R. Chowdhury, M. Ying, L. Xu, M. Li, H.-J. Chung, H. Keum, M. McCormick, P. Liu, Y.-W. Zhang, F. G. Omenetto, Y. Huang, T. Coleman, J. A. Rogers, *Science* **2011**, *333*, 838.
[62] D.-H. Kim, N. Lu, R. Ghaffari, Y.-S. Kim, S. P. Lee, L. Xu, J. Wu, R.-H. Kim, J. Song, Z. Liu, J. Viventi, B. de Graff, B. Elolampi, M. Mansour, M. J. Slepian, S. Hwang, J. D. Moss, S.-M. Won, Y. Huang, B. Litt, J. A. Rogers, *Nat. Mater.* **2011**, *10*, 316.
[63] Y. Zhang, S. Xu, H. Fu, J. Lee, J. Su, K.-C. Hwang, J. A. Rogers, Y. Huang, *Soft Matter* **2013**, *9*, 8062.
[64] T. Sekitani, Y. Noguchi, K. Hata, T. Fukushima, T. Aida, T. Someya, *Science* **2008**, *321*, 1468.
[65] T. Sekitani, H. Nakajima, H. Maeda, T. Fukushima, T. Aida, K. Hata, T. Someya, *Nat. Mater.* **2009**, *8*, 494.
[66] C.-H. Lin, D.-S. Tsai, T.-C. Wei, D.-H. Lien, J.-J. Ke, C.-H. Su, J.-Y. Sun, Y.-C. Liao, J.-H. He, *ACS Nano* **2017**, *11*, 10230.
[67] W. Wang, C. Li, H. Rodrigue, F. Yuan, M.-W. Han, M. Cho, S.-H. Ahn, *Adv. Funct. Mater.* **2017**, *27*, 1604214.
[68] Z. Wang, L. Zhang, S. Duan, H. Jiang, J. Shen, C. Li, *J. Mater. Chem. C* **2017**, *5*, 8714.
[69] C. Wu, X. Wang, L. Lin, H. Guo, Z. L. Wang, *ACS Nano* **2016**, *10*, 4652.
[70] T. Xie, *Polymer* **2011**, *52*, 4985.
[71] P. T. Mather, X. F. Luo, I. A. Rousseau, *Annu. Rev. Mater. Res.* **2009**, *39*, 445.
[72] Q. Zhao, H. J. Qi, T. Xie, *Prog. Polym. Sci.* **2015**, *49*, 79.
[73] F. Liu, M. W. Urban, *Prog. Polym. Sci.* **2010**, *35*, 3.
[74] Y. Qiu, K. Park, *Adv. Drug Delivery Rev.* **2001**, *53*, 321.
[75] M. Camacho-Lopez, H. Finkelmann, P. Palffy-Muhoray, M. Shelley, *Nat. Mater.* **2004**, *3*, 307.
[76] T. J. White, D. J. Broer, *Nat. Mater.* **2015**, *14*, 1087.
[77] C. Wei, D. Srivastava, K. Cho, *Nano Lett.* **2002**, *2*, 647.
[78] T. G. Leong, C. L. Randall, B. R. Benson, N. Bassik, G. M. Stern, D. H. Gracias, *Proc. Natl. Acad. Sci. USA* **2009**, *106*, 703.
[79] S. Felton, M. Tolley, E. Demaine, D. Rus, R. Wood, *Science* **2014**, *345*, 644.
[80] M. T. Tolley, R. F. Shepherd, M. Karpelson, N. W. Bartlett, K. C. Galloway, M. Wehner, R. Nunes, G. M. Whitesides, R. J. Wood, in *IEEE/RSJ Int. Conf. on Intelligent Robots and Systems (IROS)*, IEEE, Chicago, IL **2014**, p. 561.
[81] S. A. Zirbel, R. J. Lang, M. W. Thomson, D. A. Sigel, P. E. Walkemeyer, B. P. Trease, S. P. Magleby, L. L. Howell, *Int. J. Mech. Mater. Des.* **2013**, *135*, 111005.
[82] C. M. Yakacki, R. Shandas, C. Lanning, B. Rech, A. Eckstein, K. Gall, *Biomaterials* **2007**, *28*, 2255.
[83] Y. Q. Mao, Z. Ding, C. Yuan, S. G. Ai, M. Isakov, J. T. Wu, T. J. Wang, M. L. Dunn, H. J. Qi, *Sci Rep* **2016**, *6*, 31110.
[84] M. Behl, M. Y. Razzaq, A. Lendlein, *Adv. Mater.* **2010**, *22*, 3388.
[85] J. Sun, Q. H. Guan, Y. J. Liu, J. S. Leng, *J. Intell. Mater. Syst. Struct.* **2016**, *27*, 2289.
[86] C. Wischke, A. T. Neffe, A. Lendlein, *Adv. Polym. Sci.* **2010**, *226*, 177.
[87] A. Lendlein, M. Behl, B. Hiebl, C. Wischke, *Expert Rev. Med. Devices* **2010**, *7*, 357.
[88] M. Behl, K. Kratz, J. Zotzmann, U. Nochel, A. Lendlein, *Adv. Mater.* **2013**, *25*, 4466.
[89] J. Zhou, S. S. Sheiko, *J. Polym. Sci., Part B: Polym. Phys.* **2016**, *54*, 1365.
[90] I. Bellin, S. Kelch, R. Langer, A. Lendlein, *Proc. Natl. Acad. Sci. USA* **2006**, *103*, 18043.
[91] H. Z. Li, X. Gao, Y. W. Luo, *Soft Matter* **2016**, *12*, 3226.
[92] J. T. Wu, C. Yuan, Z. Ding, M. Isakov, Y. Q. Mao, T. J. Wang, M. L. Dunn, H. J. Qi, *Sci Rep* **2016**, *6*, 24224.
[93] Y. Liu, J. K. Boyles, J. Genzer, M. D. Dickey, *Soft Matter* **2012**, *8*, 1764.
[94] M. N. Robin, C. Jianguo, G. Xiaogang, Z. Fenghua, W. Wenxin, D. Yousef, S. Fabrizio, L. Jinsong, P. Hua-Xin, *Smart Mater. Struct.* **2017**, *26*, 05LT03.
[95] Y. Tang, G. Lin, S. Yang, Y. K. Yi, R. D. Kamien, J. Yin, *Adv. Mater.* **2017**, *29*, 1604262.
[96] Q. Zhao, W. K. Zou, Y. W. Luo, T. Xie, *Sci. Adv.* **2016**, *2*, e1501297.
[97] N. Zheng, Z. Fang, W. Zou, Q. Zhao, T. Xie, *Angew. Chem., Int. Ed.* **2016**, *55*, 11421.
[98] Y. Liu, B. Shaw, M. D. Dickey, J. Genzer, *Sci. Adv.* **2017**, *3*, e1602417.

[99] K. Yu, A. Ritchie, Y. Mao, M. L. Dunn, H. J. Qi, *Proc. Iutam* **2015**, *12*, 193.
[100] Y. Mao, K. Yu, M. S. Isakov, J. Wu, M. L. Dunn, H. J. Qi, *Sci. Rep.* **2015**, *5*, 13616.
[101] E. Hawkes, B. An, N. M. Benbernou, H. Tanaka, S. Kim, E. Demaine, D. Rus, R. J. Wood, *Proc. Natl. Acad. Sci. USA* **2010**, *107*, 12441.
[102] S. M. Felton, M. T. Tolley, B. Shin, C. D. Onal, E. D. Demaine, D. Rus, R. J. Wood, *Soft Matter* **2013**, *9*, 7688.
[103] K. E. Laflin, C. J. Morris, T. Muqeem, D. H. Gracias, *Appl. Phys. Lett.* **2012**, *101*, 131901.
[104] B. G. Chung, K.-H. Lee, A. Khademhosseini, S.-H. Lee, *Lab Chip* **2012**, *12*, 45.
[105] J. L. Drury, D. J. Mooney, *Biomaterials* **2003**, *24*, 4337.
[106] O. Wichterle, D. Lim, *Nature* **1960**, *185*, 117.
[107] W. Bian, B. Liau, N. Badie, N. Bursac, *Nat. Protoc.* **2009**, *4*, 1522.
[108] C. Ma, T. Li, Q. Zhao, X. Yang, J. Wu, Y. Luo, T. Xie, *Adv. Mater.* **2014**, *26*, 5665.
[109] Z. C. Eckel, C. Y. Zhou, J. H. Martin, A. J. Jacobsen, W. B. Carter, T. A. Schaedler, *Science* **2016**, *351*, 58.
[110] S. M. Hong, D. Sycks, H. F. Chan, S. T. Lin, G. P. Lopez, F. Guilak, K. W. Leong, X. H. Zhao, *Adv. Mater.* **2015**, *27*, 4035.
[111] A. S. Gladman, E. A. Matsumoto, R. G. Nuzzo, L. Mahadevan, J. A. Lewis, *Nat. Mater.* **2016**, *15*, 413.
[112] Q. Ge, H. J. Qi, M. L. Dunn, *Appl. Phys. Lett.* **2013**, *103*, 131901.
[113] L. M. Huang, R. Q. Jiang, J. J. Wu, J. Z. Song, H. Bai, B. G. Li, Q. Zhao, T. Xie, *Adv. Mater.* **2017**, *29*, 1605390.
[114] S. Xu, Z. Yan, K. I. Jang, W. Huang, H. R. Fu, J. Kim, Z. Wei, M. Flavin, J. McCracken, R. Wang, A. Badea, Y. Liu, D. Q. Xiao, G. Y. Zhou, J. Lee, H. U. Chung, H. Y. Cheng, W. Ren, A. Banks, X. L. Li, U. Paik, R. G. Nuzzo, Y. G. Huang, Y. H. Zhang, J. A. Rogers, *Science* **2015**, *347*, 154.
[115] Y. H. Zhang, Z. Yan, K. W. Nan, D. Q. Xiao, Y. H. Liu, H. W. Luan, H. R. Fu, X. Z. Wang, Q. L. Yang, J. C. Wang, W. Ren, H. Z. Si, F. Liu, L. H. Yang, H. J. Li, J. T. Wang, X. L. Guo, H. Y. Luo, L. Wang, Y. G. Huang, J. A. Rogers, *Proc. Natl. Acad. Sci. USA* **2015**, *112*, 11757.
[116] Z. Yan, F. Zhang, J. C. Wang, F. Liu, X. L. Guo, K. W. Nan, Q. Lin, M. Y. Gao, D. Q. Xiao, Y. Shi, Y. T. Qiu, H. W. Luan, J. H. Kim, Y. Q. Wang, H. Y. Luo, M. D. Han, Y. G. Huang, Y. H. Zhang, J. A. Rogers, *Adv. Funct. Mater.* **2017**, *26*, 2629.
[117] Z. Yan, M. D. Han, Y. Shi, A. Badea, Y. Y. Yang, A. Kulkarni, E. Hanson, M. E. Kandel, X. W. Wen, F. Zhang, Y. Y. Luo, Q. Lin, H. Zhang, X. G. Guo, Y. M. Huang, K. W. Nan, S. Jia, A. W. Oraham, M. B. Mevis, J. M. Lim, X. L. Guo, M. Y. Gao, W. Ryu, K. J. Yu, B. G. Nicolau, A. Petronico, S. S. Rubakhin, J. Lou, P. M. Ajayan, K. Thornton, G. Popescu, D. N. Fang, J. V. Sweedler, P. V. Braun, H. X. Zhang, R. G. Nuzzo, Y. G. Huang, Y. H. Zhang, J. A. Rogers, *Proc. Natl. Acad. Sci. USA* **2017**, *114*, E9455.
[118] Z. C. Fan, K. C. Hwang, J. A. Rogers, Y. G. Huang, Y. H. Zhang, *J. Mech. Phys. Solids* **2018**, *111*, 215.
[119] Y. Liu, Z. Yan, Q. Lin, X. L. Guo, M. D. Han, K. Nan, K. C. Hwang, Y. G. Huang, Y. H. Zhang, J. A. Rogers, *Adv. Funct. Mater.* **2016**, *26*, 2909.
[120] R. Xu, R. Li, Z. Du, W. Zhang, Y. Zhu, Z. Sun, X. Guo, *Extreme Mech. Lett.* **2017**, *15*, 139.
[121] Z. Yan, F. Zhang, J. C. Wang, F. Liu, X. L. Guo, K. W. Nan, Q. Lin, M. Y. Gao, D. Q. Xiao, Y. Shi, Y. T. Qiu, H. W. Luan, J. H. Kim, Y. Q. Wang, H. Y. Luo, M. D. Han, Y. G. Huang, Y. H. Zhang, J. A. Rogers, *Adv. Funct. Mater.* **2016**, *26*, 2629.
[122] D. M. Sussman, Y. Cho, T. Castle, X. T. Gong, E. Jung, S. Yang, R. D. Kamien, *Proc. Natl. Acad. Sci. USA* **2015**, *112*, 7449.
[123] L. H. Dudte, E. Vouga, T. Tachi, L. Mahadevan, *Nat. Mater.* **2016**, *15*, 583.
[124] Z. Yan, F. Zhang, F. Liu, M. Han, D. Ou, Y. Liu, Q. Lin, X. Guo, H. Fu, Z. Xie, M. Gao, Y. Huang, J. Kim, Y. Qiu, K. Nan, J. Kim, P. Gutruf, H. Luo, A. Zhao, K.-C. Hwang, Y. Huang, Y. Zhang, J. A. Rogers, *Sci. Adv.* **2016**, *2*, e1601014.
[125] K.-I. Jang, K. Li, H. U. Chung, S. Xu, H. N. Jung, Y. Yang, J. W. Kwak, H. H. Jung, J. Song, C. Yang, A. Wang, Z. Liu, J. Y. Lee, B. H. Kim, J.-H. Kim, J. Lee, Y. Yu, B. J. Kim, H. Jang, K. J. Yu, J. Kim, J. W. Lee, J.-W. Jeong, Y. M. Song, Y. Huang, Y. Zhang, J. A. Rogers, *Nat. Commun.* **2017**, *8*, 15894.
[126] K. Nan, H. Luan, Z. Yan, X. Ning, Y. Wang, A. Wang, J. Wang, M. Han, M. Chang, K. Li, Y. Zhang, W. Huang, Y. Xue, Y. Huang, Y. Zhang, J. A. Rogers, *Adv. Funct. Mater.* **2017**, *27*, 1604281.
[127] X. Ning, H. Wang, X. Yu, J. A. N. T. Soares, Z. Yan, K. Nan, G. Velarde, Y. Xue, R. Sun, Q. Dong, H. Luan, C. M. Lee, A. Chempakasseril, M. Han, Y. Wang, L. Li, Y. Huang, Y. Zhang, J. A. Rogers, *Adv. Funct. Mater.* **2017**, *27*, 1605914.
[128] J. M. McCracken, S. Xu, A. Badea, K.-I. Jang, Z. Yan, D. J. Wetzel, K. Nan, Q. Lin, M. Han, M. A. Anderson, J. W. Lee, Z. Wei, M. Pharr, R. Wang, J. Su, S. S. Rubakhin, J. V. Sweedler, J. A. Rogers, R. G. Nuzzo, *Adv. Biosyst.* **2017**, *1*, 1700068.
[129] H. Fu, K. Nan, P. Froeter, W. Huang, Y. Liu, Y. Wang, J. Wang, Z. Yan, H. Luan, X. Guo, Y. Zhang, C. Jiang, L. Li, A. C. Dunn, X. Li, Y. Huang, Y. Zhang, J. A. Rogers, *Small* **2017**, *13*, 1700151.
[130] T. G. Leong, C. L. Randall, B. R. Benson, N. Bassik, G. M. Stern, D. H. Gracias, *Proc. Natl. Acad. Sci. USA* **2009**, *106*, 703.
[131] B. Tian, J. Liu, T. Dvir, L. Jin, J. H. Tsui, Q. Qing, Z. Suo, R. Langer, D. S. Kohane, C. M. Lieber, *Nat. Mater.* **2012**, *11*, 986.
[132] R. J. Wood, *Am. Sci.* **2014**, *102*, 124.
[133] D. Bishop, F. Pardo, C. Bolle, R. Giles, V. Aksyuk, *J. Low Temp. Phys.* **2012**, *169*, 386.
[134] Z. Fan, H. Razavi, J.-w. Do, A. Moriwaki, O. Ergen, Y.-L. Chueh, P. W. Leu, J. C. Ho, T. Takahashi, L. A. Reichertz, *Nat. Mater.* **2009**, *8*, 648.
[135] W. Xu, Z. Qin, C.-T. Chen, H. R. Kwag, Q. Ma, A. Sarkar, M. J. Buehler, D. H. Gracias, *Sci. Adv.* **2017**, *3*, e1701084.
[136] M. K. Blees, A. W. Barnard, P. A. Rose, S. P. Roberts, K. L. McGill, P. Y. Huang, A. R. Ruyack, J. W. Kevek, B. Kobrin, D. A. Muller, P. L. McEuen, *Nature* **2015**, *524*, 204.
[137] X. W. Yu, H. H. Cheng, M. Zhang, Y. Zhao, L. T. Qu, G. Q. Shi, *Nat. Rev. Mater.* **2017**, *2*, 17046.
[138] G. R. Bhimanapati, Z. Lin, V. Meunier, Y. Jung, J. Cha, S. Das, D. Xiao, Y. Son, M. S. Strano, V. R. Cooper, L. B. Liang, S. G. Louie, E. Ringe, W. Zhou, S. S. Kim, R. R. Naik, B. G. Sumpter, H. Terrones, F. N. Xia, Y. L. Wang, J. Zhu, D. Akinwande, N. Alem, J. A. Schuller, R. E. Schaak, M. Terrones, J. A. Robinson, *ACS Nano* **2015**, *9*, 11509.
[139] H. Jang, Y. J. Park, X. Chen, T. Das, M. S. Kim, J. H. Ahn, *Adv. Mater.* **2016**, *28*, 4184.
[140] R. Raccichini, A. Varzi, S. Passerini, B. Scrosati, *Nat. Mater.* **2015**, *14*, 271.
[141] W. Lv, Z. J. Li, Y. Q. Deng, Q. H. Yang, F. Y. Kang, *Energy Storage Mater.* **2016**, *2*, 107.
[142] E. Pomerantseva, Y. Gogotsi, *Nat. Energy* **2017**, *2*, 17089.
[143] R. Kurapati, K. Kostarelos, M. Prato, A. Bianco, *Adv. Mater.* **2017**, *29*, 1700909.